CrossMark

3-Bromopyruvate induces rapid human prostate cancer cell death by affecting cell energy metabolism, GSH pool and the glyoxalase system

Daniela Valenti[1] · Rosa A. Vacca[1] · Lidia de Bari[1]

Abstract 3-bromopyruvate (3-BP) is an anti-tumour drug effective on hepatocellular carcinoma and other tumour cell types, which affects both glycolytic and mitochondrial targets, depleting cellular ATP pool. Here we tested 3-BP on human prostate cancer cells showing, differently from other tumour types, efficient ATP production and functional mitochondrial metabolism. We found that 3-BP rapidly induced cultured androgen-insensitive (PC-3) and androgen-responsive (LNCaP) prostate cancer cell death at low concentrations (IC_{50} values of 50 and 70 μM, respectively) with a multimodal mechanism of action. In particular, 3-BP-treated PC-3 cells showed a selective, strong reduction of glyceraldeide 3-phosphate dehydrogenase activity, due to the direct interaction of the drug with the enzyme. Moreover, 3-BP strongly impaired both glutamate/malate- and succinate-dependent mitochondrial respiration, membrane potential generation and ATP synthesis, concomitant with the inhibition of respiratory chain complex I, II and ATP synthase activities. The drastic reduction of cellular ATP levels and depletion of GSH pool, associated with significant increase in cell oxidative stress, were found after 3-BP treatment of PC-3 cells. Interestingly, the activity of both glyoxalase I and II, devoted to the elimination of the cytotoxic methylglyoxal, was strongly inhibited by 3-BP. Both N-acetylcysteine and aminoguanidine, GSH precursor and methylglyoxal scavenger, respectively, prevented 3-BP-induced PC-3 cell death, showing that impaired cell antioxidant and detoxifying capacities are crucial events leading to cell death. The provided information on the multi-target

cytotoxic action of 3-BP, finally leading to PC-3 cell necrosis, might be useful for future development of 3-BP as a therapeutic option for prostate cancer treatment.

Keywords PC-3 cells · LNCaP cells · 3-bromopyruvate · Glycolysis · Mitochondrial bioenergetics · Glyoxalase system

Abbreviations

AA	Antimycin A
AG	Aminoguanidine
Ap5A	P1,P5-Di(adenosine-5′) pentaphosphate
ASC	Ascorbate
3-BP	3-bromopyruvate
cHK	Cytosolic hexokinase
CN^-	Potassium cyanide
CSF	Cell soluble fraction
DCF	Dichlorofluorescein
DCFH-DA	2′,7′-dichlorofluorescein diacetate
DCIP	Dichloroindophenol
FCCP	Carbonylcyanide p-trifluoromethoxyphenylhydrazone
GAPDH	Glyceraldeide 3-phosphate dehydrogenase
GLOI, GLOII	Glyoxalase I, glyoxalase II
G6P-DH	Glucose-6-phosphate dehydrogenase
GLU	Glutamate
GSH	Reduced glutathione
HK	Hexokinase
L-LDH	L-lactate dehydrogenase
MAL	Malate
MG	Methylglyoxal
mHK	Mitochondrial membrane-associated hexokinase
MMEF	Mitochondrial membrane enriched fraction

✉ Lidia de Bari
l.debari@ibbe.cnr.it

[1] Istituto di Biomembrane e Bioenergetica, Consiglio Nazionale delle Ricerche, Via G. Amendola, 165/A, 70126 Bari, Italy

⚛ Springer

MRC	Mitochondrial respiratory chain
NAC	N-acetylcysteine
OLIGO	Oligomycin
OXPHOS	Oxidative phosphorylation
PK	Pyruvate kinase
pPC-3	Digitonin-permeabilized PC-3 cells
ROS	Reactive oxygen species
ROT	Rotenone
SUCC	Succinate
TMPD	N,N,N',N'-tetramethyl-p-phenylenediamine
XTT	3-(4,5-dimethylthiazol-2-yl)-2,5-diphenyltetrazolium bromide

Introduction

3-Bromopyruvic acid (3-BP) is an alkylating agent with high reactivity for -SH and -OH protein groups, discovered by Ko et al. (2001) as potent anticancer agent and reported to be effective in eradicating hepatocellular carcinoma, without affecting healthy surrounding tissues (Geschwind et al. 2002; Ko et al. 2004). 3-BP has been shown to be a potent inhibitor of ATP production by affecting both glycolytic and mitochondrial targets (Ko et al. 2004; Pereira da Silva et al. 2009; Amoêdo et al. 2013) and to cause GSH depletion and oxidative stress increase (Sadowska-Bartosz and Bartosz 2013; Ehrke et al. 2015). In particular, key enzymes of energy metabolism known to be targets of 3-BP include the mitochondrial hexokinase and glyceraldeide 3-phosphate dehydrogenase (GAPDH) in the glycolytic pathway, and mitochondrial succinate dehydrogenase (Shoshan 2012). Interestingly, a patented formulation of 3-BP has been recently employed for the delivery in humans and shown to cause very rapid fibrolamellar hepatocellular carcinoma necrosis with low side effects (Ko et al. 2012).

Differently from many tumours in which the activation of aerobic glycolysis and down-regulation of oxidative phosphorylation (OXPHOS) take place, as originally proposed by Warburg (Koppenol et al. 2011), human prostate cancer cells show glycolysis comparable to normal prostate cells, enhanced fatty acid oxidation and a functional Krebs cycle, bringing to efficient ATP production (Liu 2006; Franklin and Costello 2007). Furthermore, enhanced mitochondrial oxidation of D-lactate (D-LAC), the final product of the methylglyoxal (MG) pathway, has been shown to contribute to ATP production in cultured prostate cancer cells (de Bari et al. 2013). Interestingly, due to their high efficiency in producing ATP, the highly metastatic, androgen-insensitive prostate cancer PC-3 cells have been shown to survive to drugs which affect either glycolysis or OXPHOS, this suggesting that the control of prostate tumour growth would require the inhibition of both ATP-producing pathways *in vivo* (Matheson et al. 2007). Thus, the possibility to inhibit at the same time glycolysis and mitochondrial functions by using a single drug is intriguing for the treatment of prostate cancer.

The MG pathway has a prominent role in the survival of prostate cancer cells (Antognelli et al. 2012; Antognelli et al. 2013); it converts the GSH-MG hemithioacetal formed from the non-enzymatic reaction between reduced glutathione (GSH) and the cytotoxic, highly reactive MG, into the non toxic D-LAC, by the combined action of glyoxalase I (GLOI, EC 4.4.1.5) and glyoxalase II (GLOII, EC 3.1.2.6) (Kalapos 1999). Since MG is mainly formed both enzymatically and non-enzymatically from the glycolytic intermediates glyceraldehyde 3-phosphate and dihydroxyacetone phosphate (Kalapos 1999), glyoxalases play a critical detoxifying role in strict connection with glycolysis, to maintain cellular activity and viability of prostatic cancer cells (Davidson et al. 2002). Interestingly, the level of both the above glycolytic intermediates was found increased in 3-BP-treated HepG2 cells, likely due to GAPDH activity impairment (Pereira da Silva et al. 2009), this being a condition favouring MG formation (Thornalley et al. 2001; Ahmed et al. 2003). At present whether 3-BP might also affect cell ability to detoxify MG through the MG pathway has never been investigated.

This prompted us to check whether, and through which mechanisms, 3-BP could affect the growth of both the invasive PC-3 cells and the poorly aggressive, androgen-responsive prostate cancer (LNCaP) cells. We show that 3-BP can rapidly cause the death of both cell types at micromolar concentrations, with the PC-3 cells being more sensitive than LNCaP cells. We found an early significant 3-BP-dependent impairment of both glycolytic GAPDH activity and mitochondrial functions, leading to a remarkable reduction of whole cell ATP level. On the other hand, 3-BP-dependent impairment of the PC-3 cell antioxidant capacity due to cell GSH pool depletion was found. Interestingly, we first show that 3-BP treatment causes the inhibition of the activity of both GLOI and GLOII, this possibly resulting in the impairment of cell detoxifying capacity contributing to cell death.

Materials and methods

Cell cultures and materials

LNCaP and PC-3 cells were obtained from the European Collection of Cell Cultures (ECACC Salisbury, UK). Cell lines were cultured at 37 °C in a humidified atmosphere with 5 % CO_2 in RPMI-1640 medium (GIBCO/BRL) supplemented with 10 % inactivated fetal bovine serum (GIBCO/BRL), 2 mM glutamine, penicillin (100 units/ml) and streptomycin (100 μg/ml) (GIBCO/BRL). Both PC-3 and LNCaP cells were collected by trypsinization, washed with phosphate buffered saline (PBS) medium containing 138 mM NaCl, 2.7 mM

KCl, 8 mM Na_2HPO_4, 15 mM KH_2PO_4 (pH 7.4) and then seeded at a density of 1.2×10^5 cells/ml into 15 or 10 cm Petri dishes or in 96-well plates. Cells were cultured for about 24 h to obtain 70–80 % confluence, before being incubated with 3-BP.

All reagents used were from Sigma-Aldrich unless otherwise specified.

3-Bromopyruvate treatment and cell proliferation assay

Soon before the experiment, 3-BP was weighted and dissolved in cold cell culture medium to a final concentration of 50 mM, and then rapidly diluted in the same medium to obtain the reported final 3-BP micromolar concentrations used to replace the medium from each plate/well with seeded cells. Untreated control cells were obtained by replacing the cell culture medium without 3-BP. Both 3-BP treated and time-matched control cells were then incubated at 37 °C for the reported incubation times. In the case of 48 h of incubation, the 3-BP-containing medium was replaced after 24 h of incubation. Where indicated, cells were incubated in N-acetylcysteine (NAC, 1 mM)- or aminoguanidine (AG, 0.5 mM)-containing medium for 30 min or 1 h, respectively, essentially as in (Qin et al. 2010; de Arriba et al. 2007), then replaced with 3-BP (50 μM)-containing or 3-BP-free (controls) medium, for the indicated times.

Cell proliferation assay was performed by using 3-(4,5-dimethylthiazol-2-yl)-2,5-diphenyltetrazolium bromide reagent (XTT, Cell Proliferation Kit II, Roche), as in Valenti et al. (2013). Cells were seeded into a 96-well plate and incubated over-night at 37 °C in a CO_2 incubator to allow adherence. XTT labelling mixture were added to each well and the plate incubated at 37 °C for 2–4 h following the manufacturer's instructions. Metabolically active cells produce a formazan dye which can be detected by measuring the increase in absorbance at the measurement/reference wavelengths of 490/655 nm, respectively.

For cell count experiments, cells were seeded in 10 cm Petri dishes, incubated over-night at 37 °C and then trypsinized, stained with Trypan blue and counted in a Bürker haemocytometer within 5 min after staining (Valenti et al. 2013).

Cell permeabilization and isolation of the mitochondrial membrane enriched fraction (MMEF) and the cell soluble fraction (CSF)

Digitonin-permeabilized PC-3 cells (pPC-3) were obtained by adding digitonin (0.01 % w/v) to cell suspension for 5 min, at room temperature. MMEF and CSF were prepared as in de Bari et al. (2013). Briefly, trypsinized PC-3 cells were precipitated by centrifugation (1300 g for 3 min, 4 °C) and washed with PBS. The cellular pellet ($4–6 \times 10^6$ cells) was dried and

frozen at −80 °C to favour cell membranes rupture, suspended in about 1 ml (final density of about 5×10^6 cells/ml) of ipotonic medium consisting of 10 mM Tris/HCl (pH 7.5) plus 1 mg/ml BSA and exposed to ultrasound energy for 15 s at 0 °C (Valenti et al. 2010). The ultrasound-treated cells were centrifuged at 1500 g for 5 min at 4 °C to remove intact cells, cellular debris and nuclei (pellet) and the supernatant was subsequently centrifuged at 18,000 g for 15 min at 4 °C. The resulting supernatant represents the CSF (about 1.2 mg protein/ml). The pellet was washed twice with 1 ml of cold PBS to eliminate any CSF contamination. The final pellet (MMEF) was suspended in 0.5 ml of respiration medium consisting of 210 mM mannitol, 70 mM sucrose, 0.1 mM EDTA, 20 mM Tris-HCl pH 7.4, 3 mM $MgCl_2$, 5 mM KH_2PO_4/K_2HPO_4 (pH 7.5) plus 1 mg/ml BSA, and used for the experiments. In each experiment, the absence of cytosolic contamination of MMEF was confirmed by assaying as in (Lohr and Waller 1963), the activity of the cytosolic marker enzyme glucose-6P-dehydrogenase (G6PDH), previously found to be not affected by 3-BP treatment (not shown).

Measurement of enzyme activities

The activity of the cytosolic HK (cHK), GAPDH, PK, L-LDH, GLOI and GLOII was measured in CSF (from 0.04 to 0.06 mg of protein), whereas the mitochondrial membrane-associated HK (mHK) activity was first assayed in MMEF (0.025 mg of protein), obtained from PC-3 cells incubated in the absence (controls) or presence of 3-BP (50 μM) at 37 °C for the reported incubation times, essentially as in (Principato et al. 1987; Kawatani et al. 2008; Higgins et al. 2009), but with some modifications. All the enzymatic activities were measured photometrically by means of a JascoV-550 spectrophotometer, at 25 °C, in a final volume of 1 ml of either respiration medium (pH 7.4) for PK, standard medium consisting of 0.3 M sucrose, 10 mM KCl, 1 mM $MgCl_2$, and 20 mM Hepes-Tris (pH 7.0) for GLOI, GLOII, L-LDH and HK, or phosphate buffer 100 mM (pH 7.4) for GAPDH. The following reaction mixtures were used: ADP (1 mM), NADH (0.2 mM) and L-LDH from rabbit muscle (5 e.u.) for PK detection; GSH (1 mM) and MG (3 mM) for GLOI detection; 5,50-dithiobis-2-nitrobenzoic acid (DTNB, 0.2 mM) for GLOII detection; NADH (0.2 mM) for L-LDH detection; $MgCl_2$ (10 mM), G6PDH from baker's yeast (S. cerevisiae) (1 e.u.), $NADP^+$ (0.25 mM) and glucose (10 mM) for HK detection; NAD^+ (1 mM), ADP (1 mM), diadenosine pentaphosphate (Ap5A, 10 μM), inhibitor of adenylate kinase, and 3-phosphoglyceric phosphokinase from rabbit muscle (15 e.u.) for GAPDH detection. Enzyme reactions were started by the addition of: 1 mM phosphoenolpyruvate (PK), 20–30 μl CSF (0.04 mg protein) (GLOI); 0.5 mM S-D-lactoylglutathione (GLOII); 1 mM pyruvate (L-LDH); 1 mM ATP (HK), 3 mM glyceraldehyde 3-phosphate (GAPDH). For

PK, L-LDH, HK and GAPDH activity, the absorbance of NAD(P)H at 340 nm was measured as a function of time ($\varepsilon_{340nm} = 6.22$ mM$^{-1} \times$ cm^{-1}). GLOI and GLOII activities were measured as rates of absorbance increase due to S-D-lactoylglutathione ($\varepsilon_{240nm} = 2.5$ mM$^{-1} \times$ cm^{-1}) and thionitrobenzoic acid ($\varepsilon_{412nm} = 13.9$ mM$^{-1} \times$ cm^{-1}) formation at 240 nm and 412 nm, respectively.

Measurement of oxygen consumption rate in pPC-3

Oxygen consumption rate was measured at 37 °C using a Gilson 5/6 oxygraph equipped with a Clark electrode. PC-3 cells, seeded in 15 cm Petri plates, were incubated in the absence or presence of 3-BP and then trypsinized, precipitated by centrifugation (1300 g for 3 min, 4 °C), washed with PBS and finally suspended in 1 ml of respiration medium (pH 7.4) at room temperature. Then 1 mg of cell protein was added to the polarographic cuvette and the volume adjusted to 1 ml with respiration medium. Cells were then permeabilized by the addition of digitonin (0.01 % w/v) for 5 min and subsequently added with the uncoupler FCCP (1.25 μM) to obtain uncoupled state 3 of respiration, a condition in which the rate of oxygen consumption is controlled exclusively by substrate oxidation and thus allows to detect dysfunction in respiratory chain components (Brand and Nicholls 2011). The respiratory substrates glutamate (GLU) plus malate (MAL) (5 mM each), SUCC (5 mM), or ascorbate (ASC, 5 mM) plus TMPD (0.5 mM) and the inhibitors rotenone (ROT, 5 μg/10 μl), antimycin A (AA, 2 μg/10 μl) and potassium cyanide (CN$^-$, 0.5 mM) were added in the sequence reported in Fig. 3a. The sensitivity of the instrument was set to allow rates of oxygen consumption as low as 0.2 natom O/min x mg protein to be measured. The rate of oxygen consumption, obtained from the tangent to the initial part of the progress curve, was expressed as natom O/min x mg cell protein.

Measurement of mitochondrial membrane potential generation

Mitochondrial membrane potential ($\Delta\psi$) generation was measured at 37 °C by monitoring the fluorescence changes of the probe safranin O at 520 nm excitation and 570 nm emission wavelengths, essentially as in (de Bari et al. 2013). PC-3 cells were cultured in 15 cm Petri plates either in the absence or presence of 3-BP and then trypsinized, precipitated and suspended in 1 ml of standard medium (pH 7.0), at room temperature. Then cells (1 mg protein) were added to the experimental cuvette in the presence of 10 μM safranin O, digitonin (0.01 % w/v) and ADP (0.5 mM), to a final volume of 2 ml of standard medium (pH 7.0). After 5 min, GLU plus MAL (5 mM each) or ROT (5 μg/10 μl) plus SUCC (5 mM) were added to start $\Delta\psi$ generation, finally abolished by the uncoupler FCCP (1.25 μM).

Determination of mitochondrial ATP production rate

The rate of appearance of the ATP produced via OXPHOS was determined spectrophotometrically in pPC-3 cells, essentially as described in (Valenti et al. 2010). Samples (0.25 mg of cell protein) were suspended at 37 °C in 2 ml of respiration medium (pH 7.4) containing the ATP detecting system (ATP-ds) consisting of glucose (2.5 mM), HK (2 e.u.), G6PDH (1 e.u.) and NADP$^+$ (0.2 mM), plus Ap5A (10 μM), used to specifically inhibit adenylate kinase, in the presence of either MAL plus GLU (5 mM each) or SUCC (5 mM) plus ROT (3 μM), as energy sources. After 5 min of incubation with 0.01 % w/v digitonin, ADP (0.5 mM) was added to start the reaction. NADPH formation, which reveals ATP appearance in the extramitochondrial phase, was monitored as absorbance increase at 340 nm. As a control, the ATP synthase inhibitor oligomycin (OLIGO, 5 μg/10 μl) was added in course of reaction to show the inhibition of the mitochondrial ATP production. HK/G6PDH coupled enzymes were added in large excess to ensure a non-limiting ADP-regenerating system for the measurement of ATP efflux. The rate of ATP appearance was measured from the tangent to the initial part of the progress curve and expressed as nmol NADPH formed/min x mg protein.

Measurement of cell ATP content

PC-3 cells seeded in 10 cm plates were incubated either in the absence or presence of 3-BP, trypsinized, collected, washed and suspended in PBS and an aliquot used for protein assay. Cells were then precipitated and finally dissolved in 0.5 ml of boiling water to obtain cell extracts, as described in (Yang et al. 2002). Cell ATP content was assayed fluorimetrically ($\lambda_{ex-em} = 334$–456 nm) at 25 °C, incubating cell extracts (250 μl) in a final volume of 2 ml of standard medium, in the presence of ATP-ds, as described in (Valenti et al. 2010). The amount of cell ATP was expressed as nmol NADPH formed/mg cell protein.

MRC complex activities assay

Measurements of MRC complex activities was performed in MMEF (0.3–0.5 mg of protein) from PC-3 cells cultured in 10 cm Petri plates. Cells were incubated either in the absence or presence of 50 μM 3-BP and collected after 3 h of incubation. Three photometric assays which rely on the sequential addition of reagents to measure the activities of: i) NADH:ubiquinone oxidoreductase (complex I) followed by ATP synthase (complex V), ii) succinate:ubiquinone oxidoreductase (complex II) and iii) cytochrome c oxidase (complex IV) followed by cytochrome c oxidoreductase (complex III), were carried out, essentially as in (Bénit et al. 2006). The

specific activities of MRC complexes were expressed as nmol/min x mg protein.

Measurement of reduced glutathione (GSH)

Intracellular GSH was detected photometrically, at 240 nm, in CSF obtained from 3-BP-treated or untreated PC-3 cells, in the presence of glyoxalase I (1 e.u.) and MG (2 mM), essentially as described in (Bobba et al. 2013). CSF (0.05–0.07 mg) was incubated at 25 °C in standard medium (pH 7.0) to a final volume of 1 ml. The amount of cell GSH was expressed as nmol GSH/mg of CSF protein. Detectable oxidized glutathione (GSSG) in CSF, assayed as (Bobba et al. 2013), was not significantly lowered after incubation with 50 μM 3-BP (data not shown); on the contrary, when 3-BP (50 μM) was added to CSF of PC-3 control cells for 5 min, cell GSH was no longer detectable this confirming the high reactivity of 3-BP toward thiols (Shoshan 2012; Ehrke et al. 2015) (not shown).

Cell reactive oxygen species (ROS) evaluation

Quantitative analysis of intracellular ROS levels was performed fluorimetrically by means of an LS50 Perkin Elmer spectrofluorimeter, by using the non-fluorescent dye 2′,7′-dichlorofluorescein diacetate (DCFH-DA) which produces the fluorescent product dichlorofluorescein (DCF) by reaction with cell ROS, mainly H_2O_2 (LeBel et al. 1992). Cultured PC-3 cells were incubated with 20 μM DCFH-DA for 30 min under growth conditions, washed twice in PBS, and collected. Then the fluorescence of the sample (100 μg of cell proteins) was recorded at the excitation-emission wavelengths of 488–520 nm, respectively, at 25 °C, in a final volume of 2 ml of PBS and expressed as arbitrary units (a.u.).

Apoptosis and necrosis assessment

Cells were seeded in 96-well culture plates, incubated for 24 h at 37 °C in a CO_2 incubator to allow adherence, and then exposed to 3-BP at the indicated concentrations for an additional 24 h time period. Apoptosis and necrosis were measured by the Cell Death ELISA[PLUS] photometric enzyme-immunoassay (Version 11.0, ROCHE), according to the manufacturer's protocol, by monitoring the absorbance at the measurement-reference wavelengths of 405–655 nm, respectively, reflecting the amount of histone-complexed DNA fragments out of cell cytoplasm after the induction of apoptosis, or when released from necrotic cells.

Released L-lactate dehydrogenase activity was measured photometrically at 340 nm, essentially as described by Bernt and Bergmeyer (1963), as a marker of cell necrosis (Porcelli et al. 2015) in the culture medium of PC-3 cells (1×10^5 cells/ml culture medium) incubated either in the absence or

presence of 3-BP for increasing times. Culture medium was centrifuged (1300 g for 3 min, 4 °C) to precipitate any cell contamination; an aliquot (100 μl) of the obtained supernatant was added to a final volume of 2 ml of standard medium, at 25 °C and added with 0.2 mM NADH plus 1 mM pyruvate to start the reaction. L-LDH activity was expressed as percent of L-LDH activity released by 3-BP-treated cells at 24 h (100 %). In untreated PC-3 cell culture medium, L-LDH activity was negligible up to 24 h (not shown).

Statistical analysis

All experiments were performed at least in triplicate and results expressed as mean ± standard deviation (SD). Statistical evaluation was performed by Student's t-test. The threshold for statistical significance was set to $P < 0.05$.

Results

3-BP inhibits prostate cancer cell growth in a dose- and time-dependent manner

In order to ascertain whether and how 3-BP can affect prostate cancer cell growth, we examined the dose-response effect of 3-BP treatment on both PC-3 and LNCaP cell proliferation, measured by Trypan Blue exclusion (Fig. 1a) and XTT (Fig. 1b) assays. PC-3 and LNCaP cells were incubated both in the absence (controls) or presence of 3-BP at increasing concentrations (25–100 μM) for 24 h. As shown in Fig. 1a and b, a dose-dependent inhibitory effect of 3-BP on both PC-3 and LNCaP cell growth was found, although the more aggressive PC-3 cells were affected by lower 3-BP concentrations than LNCaP cells, being the estimated 3-BP IC_{50} values of 50 μM and 70 μM, respectively, as measured by XXT assay. Interestingly, after 24 h-treatment with 60 μM 3-BP, while PC-3 cells were already almost all killed by the drug, the less proliferating LNCaP cell viability was decreased by only 40 % ($P < 0.01$).

We further monitored the effect of three separate 3-BP concentrations (25, 50, 100 μM) on PC-3 cell viability as a function of the incubation time (Fig. 1c and d). No significant effect on cell viability was found with 25 μM 3-BP up to 48 h of incubation, as measured by both Trypan Blue exclusion (Fig. 1c) and XTT (Fig. 1d) assays; conversely, as expected, 100 μM 3-BP killed very quickly almost all cells resulting very cytotoxic for PC-3 cells ($P < 0.01$). 3-BP at a concentration of 50 μM reduced progressively PC-3 cell viability within 48 h-incubation time, being cell growth inhibited by 35 % ($P < 0.05$) with respect to untreated controls, already after 3 h of incubation with 3-BP (Fig. 1c, d and insets). Results comparable to those reported in the inset of Fig. 1c
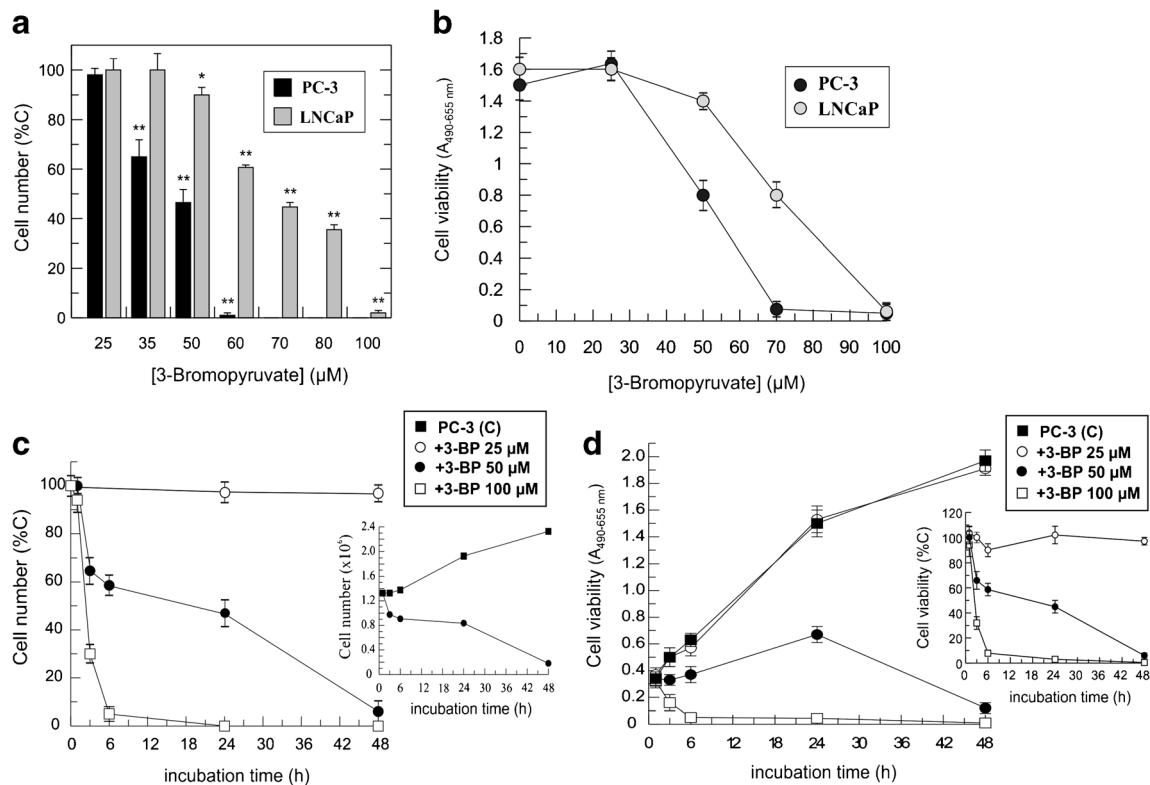
Fig. 1 Dose- and time-response effect of 3-BP on cultured human prostate cancer cell proliferation. PC-3 and LNCaP cells were incubated for 24 h both in the absence or presence of 3-BP at the reported concentrations (**a, b**). PC-3 cells were incubated for the reported times, at three different 3-BP concentrations (see box) (**c, d**). Cell number and viability were analysed by Trypan Blue exclusion (**a, c**) and XTT cell proliferation (**b, d**) assays, respectively, and expressed as either % of the values found in untreated cells (**a, c**), or absorbance at the measurement-

reference wavelengths of 490–655 nm (**b, d**). In the insets of **c** and **d** the number of PC-3 cells (× 10⁶) incubated with 3-BP (50 μM) for increasing time and XTT test results of **d** are reported as % of time-matched untreated control values (PC-3 C). All values represent means ± SD ($n = 5$), with the exception of those reported in **C inset,** in which a typical experiment is reported. ******$P < 0.01$ and *****$P < 0.05$, significantly different from untreated cells

were obtained with LNCaP cells incubated with 70 μM 3-BP as a function of time (not shown).

To check the molecular targets of 3-BP in prostate cancer cells, all further analysis made throughout this study were carried out incubating the aggressive PC-3 cells with 3-BP at a concentration of 50 μM.

3-BP effect on glycolytic enzymes in PC-3 cells

To ascertain how 3-BP cytotoxicity occurs, we assayed the activity of certain key glycolytic enzymes of PC-3 cells incubated for 24 h in the absence or presence of 3-BP (Fig. 2a). Consistently with other cancer cell lines in which GAPDH has been shown to be a target of 3-BP (Pereira da Silva et al. 2009; Ehrke et al. 2015; Ganapathy-Kanniappan et al. 2009), also in human prostate cancer PC-3 cells GAPDH activity was strongly impaired by 3-BP with respect to controls, being 58 ± 21 and 456 ± 24 nmol/min x mg protein, respectively ($P < 0.01$). On the contrary, no significant inhibition occurred in 3-BP-treated PC-3 cells, as compared to controls, in the activity of cHK (29.5 ± 1.7 and 32 ± 3.0 nmol/min x mg protein, respectively) and L-

LDH (408 ± 26 and 413 ± 20 nmol/min x mg protein, respectively). Interestingly, in good agreement with Pereira da Silva et al. (2009) and Ganapathy-Kanniappan et al. (2009), we found a 3-BP-dependent significant increase in the activity of PK (1006 ± 32.5 and 712 ± 20 nmol/min x mg protein, in 3-BP-treated and untreated cells, respectively) and mHK (70.6 ± 6.2 and 51.4 ± 5.8 nmol/min x mg protein, in 3-BP-treated and untreated cells, respectively) ($P < 0.05$).

To check whether GAPDH inhibition occurred as an early event of 3-BP cytotoxicity, the enzyme activity was monitored as a function of 3-BP incubation time (Fig. 2b). A significant inhibition by more than 90 % with respect to control activity was detected already after 3 h of incubation, remaining inhibited for the all the incubation period ($P < 0.01$). Interestingly, the activity of GAPDH of untreated PC-3 cells was also inhibited by 96 % when 3-BP (50 μM) was added to the cell soluble fraction directly into the experimental cuvette before glyceraldehyde 3-phosphate, used to start the enzyme reaction (Fig. 2c), this indicating that the inhibition of GAPDH activity is due to the direct interaction between the enzyme and the drug.
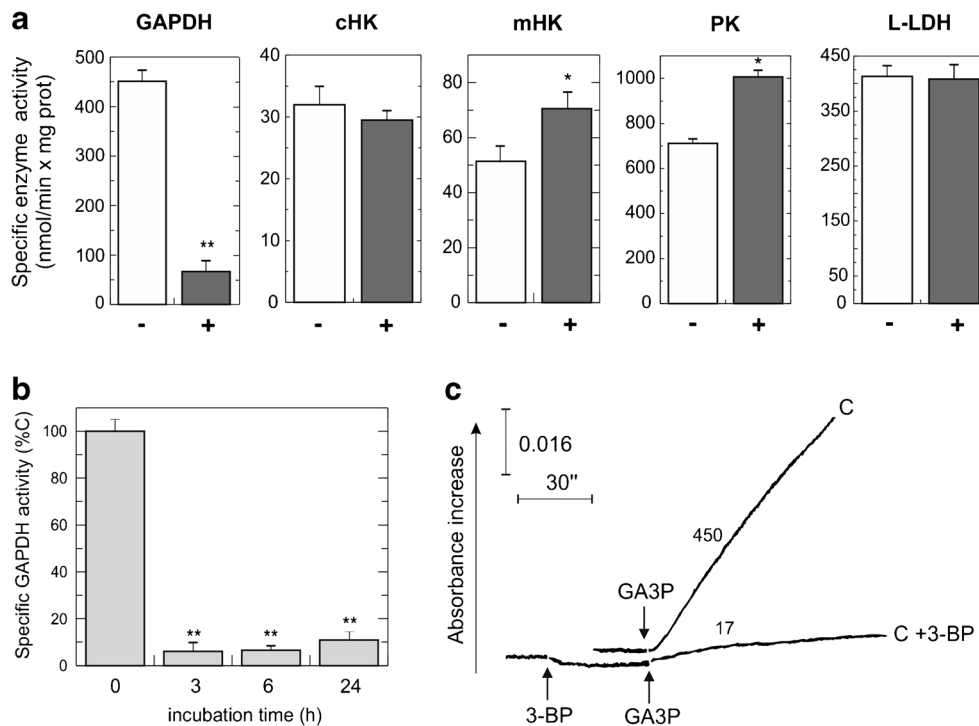
Fig. 2 The effect of 3-BP treatment of PC-3 cells on certain glycolytic enzyme activities. (**a**) The activity of cHK, mHK, GAPDH, PK and L-LDH was assayed in CSFs or MMEFs obtained from PC-3 cells incubated for 24 h either in the absence (−) or presence (+) of 50 μM 3-BP (see Materials and methods section), and expressed as nmol/min x mg protein. Values represent means ± SD (n = 5). (**b**) PC-3 cells were incubated with 3-BP (50 μM) for the indicated times. Then GAPDH activity was measured and expressed as % of the activity found in time-matched untreated controls (see Materials and methods section). Values represent means ± SD (n = 5). **P < 0.01 and *P < 0.05, significantly different from untreated cells. (**c**) GAPDH activity was assayed photometrically, at 340 nm, in CSF of untreated PC-3 cells (C, about 0.06 mg protein). Where indicated 3-BP (50 μM) was added to the experimental cuvette (C + 3-BP) before glyceraldehyde 3-phosphate (GA3P, 3 mM) which started the reaction. Numbers along traces are specific enzyme activities calculated as tangent to the initial part of the experimental trace and expressed as nmol/min × mg protein

3-BP treatment of PC-3 cells early impairs mitochondrial bioenergetics and total cell ATP level

Beside the striking inhibition of GAPDH activity, which could drastically impair the ATP harvesting stage of glycolysis, to check whether and how 3-BP could also affect mitochondrial bioenergetics, we carried out a functional study of PC-3 cell mitochondria by monitoring both respiration (Fig. 3a), Δψ generation (Fig. 3b) and rate of ATP production via OXPHOS (Fig. 3c) in pPC-3 cells incubated either in the absence (control cells, C) or presence of 3-BP (50 μM, +3-BP) for 3 h. As shown by the typical experimental traces reported in Fig. 3a, the addition of complex I substrate pair GLU/MAL caused oxygen consumption at a rate 60 % lower in +3-BP with respect to control cells (0.8 and 2.0 nat O/min x mg protein, respectively), blocked in both cell types by complex I inhibitor ROT, as expected. Similarly, the complex II substrate SUCC-dependent respiration rate was 60 % lower in +3-BP as compared to control cells (3.2 and 8.0 nat O/min × mg protein, respectively). In both cases, either AA (Fig. 3a) or malonate (5 mM) (not shown), inhibitors of complexes III and II, respectively, abolished oxygen consumption. Finally, the addition of

complex IV substrate pair ASC/TMPD induced oxygen consumption at similar rates in +3-BP and control cells (22.0 and 24.0 nat O/min x mg protein, respectively). Complex IV inhibitor CN^-, completely inhibited respiration in both cases, as expected (Fig. 3a). The statistical analysis performed on three different experiments carried out with separate cell preparations, confirmed that the rates of GLU/MAL- and SUCC-dependent respiration found in +3-BP cells (1.0 ± 0.2, 3.5 ± 0.4 nat O/min x mg protein, respectively) were significantly reduced by 56 % and 58 %, respectively as compared to control values (2.3 ± 0.2, 8.3 ± 0.5 nat O/min x mg protein, respectively) (P < 0.05), whereas the ASC/TMPD-dependent oxygen consumption rates did not differ significantly (22.0 ± 1.5 nat O/min x mg protein in +3-BP cells and 23.0 ± 1.0 nat O/min x mg protein in control cells).

In parallel, Δψ generation induced by either GLU/MAL or SUCC was measured, as illustrated by the representative experimental traces in Fig. 3b, and the mean values of Δψ extent found to be reduced by 40 ± 4 % and 60 ± 5 % (P < 0.05, n = 3), respectively, in +3-BP as compared to control cells.

Consistently with the results shown in Fig. 3a and b, suggesting the impairment of MRC complexes I and II, the mean
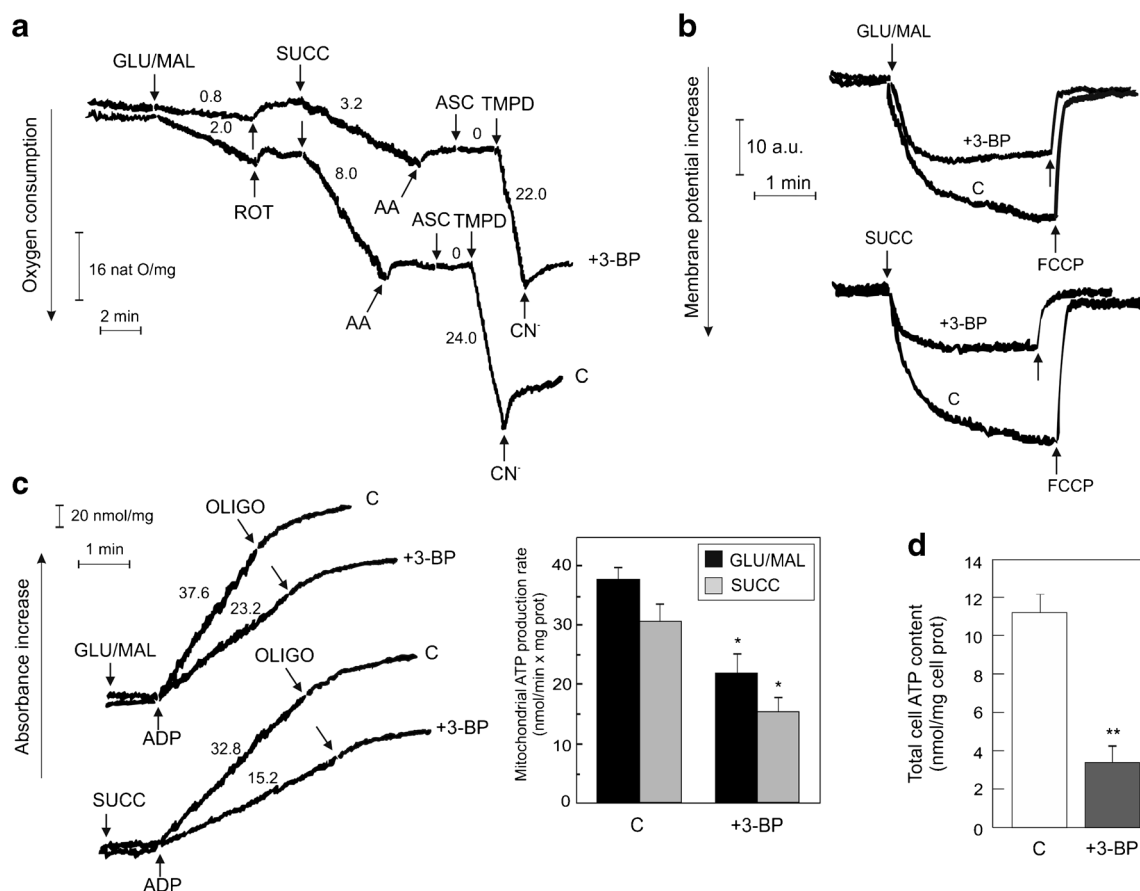
Fig. 3 The effect of 3-BP treatment on mitochondrial functions and cell energy status in PC-3 cells. Measurements of mitochondrial oxygen consumption (**a**), Δψ generation (**b**) and ATP production rate via OXPHOS (**c**) were carried out in PC-3 cells incubated either in the absence (C) or presence (+3-BP) of 50 μM 3-BP for 3 h, permeabilized with digitonin and then added with either the uncoupler FCCP (1.25 μM) (**a**), ADP (0.5 mM) (**b**), or the ATP detecting system plus Ap5A (10 μM) (**C**) (for details see the Materials and methods section). (**a**) Where indicated the following additions were made: GLU/MAL (5 mM each), ROT (5 μg/10 μl), SUCC (5 mM), AA (2 μg/10 μl), ASC (5 mM), TMPD (0.5 mM), CN⁻ (0.5 mM), FCCP (1.25 μM), ADP (0.5 mM)

and OLIGO (5 μg/10 μl). Numbers along curves are rates of oxygen consumption expressed as natO/min x mg cell protein (**b**) and of ATP appearance expressed as nmol/min x mg cell protein (**c**). Values in the histogram of **c** represent means ± SD (n = 4). *P < 0.05, significantly different from untreated cells. (**d**) Measurement of whole cell ATP level was carried out in CSFs isolated from PC-3 cells incubated either in the absence (C) or presence (+3-BP) of 50 μM 3-BP for 3 h (for details see the Materials and methods section). Values in the histogram represent means ± SD (n = 5). **P < 0.01, significantly different from untreated cells

rates of both GLU/MAL- and SUCC-dependent ATP synthesis via OXPHOS were found to be inhibited by 42 % and 50 %, respectively in +3-BP (21.7 ± 3.3 and 15.3 ± 2.4 nmol ATP/min x mg protein, respectively), as compared to control cells (37.5 ± 2.0 and 30.4 ± 3.0 nmol ATP/min x mg protein, respectively) (P < 0.05), as reported in the inset of Fig. 3c and illustrated by the representative experimental traces in Fig. 3c.

To further investigate and establish the relative contribution of each MRC complex to 3-BP-dependent impairment of mitochondrial function, all MRC complex activities were assayed in MMEF obtained from PC-3 cells incubated either in the absence (controls) or presence of 3-BP for 3 h.

The values of specific MRC complex activities, reported in Table 1, show that complex I, II, and V activities were inhibited by 25 %, 36 % and 35 %, respectively, by the drug

as compared to control activities (P < 0.05), whereas no impairment was detected in the activity of complexes III and IV.

Finally, the total cell ATP content, assayed in cell extracts obtained from 3BP-treated PC-3 cells, was found to be reduced by about 70 % (P < 0.01) after 3 h incubation with respect to untreated PC-3 cells (3.4 ± 0.8 and 11.2 ± 1.0 nmol/mg cell protein, respectively), this showing that the early 3-BP-dependent impairment of both GAPDH activity and mitochondrial bioenergetics affects the whole cell energy status (Fig. 3d).

3-BP-treatment causes early GSH depletion, ROS increase and glyoxalase system impairment in PC-3 cells

Since 3-BP can react with -SH groups, depleting GSH pool with consequent impairment of cell antioxidant defences, as

Table 1 Effect of 3-BP treatment on MRC complexes activity in PC-3 cells

	Complex I (nmol NADHox/min × mg prot)	Complex II (nmol SUCCox/min × mg prot)	Complex III (nmol cyt c red/min × mg prot)	Complex IV (nmol cyt c ox/min × mg prot)	Complex V (nmol NADHox/min × mg prot)
PC-3	6.0 ± 0.5	15.4 ± 2.0	9.9 ± 2.0	24.0 ± 2.3	17.0 ± 0.5
PC-3 + 3-BP	4.5 ± 0.3*	9.8 ± 0.4*	10.5 ± 1.8	23.8 ± 2.0	11.0 ± 0.6*

Values represent mean rates ± SD ($n = 4$). *$P < 0.05$, significantly different from untreated cells

already found in primary rat astrocytes and human erythrocytes (Sadowska-Bartosz and Bartosz 2013; Ehrke et al. 2015), PC-3 cell GSH pool was monitored as a function of 3-BP incubation time (Fig. 4a). GSH amount was strongly reduced with respect to untreated cells at all incubation times ($P < 0.01$), with the more marked decrease (about 80 %) occurring after 3 h of incubation with the drug (56.6 ± 5.3 and 10.0 ± 2.0 nmol/mg protein, in untreated and 3-BP-treated cells, respectively). In parallel, the detection of ROS production in 3-BP-treated cells revealed that, after 3 h of incubation with the drug, 55 % of increase ($P < 0.05$) in cellular ROS level occurred, as compared to control level, as shown by DCF fluorescence increase (Fig. 4b). Interestingly, pretreatment of PC-3 cells with NAC, which is taken up by PC-3 cells and converted to GSH (Weiss et al. 2015), counteracted both 3-BP-dependent GSH pool depletion (Fig. 4a) and ROS overproduction (Fig. 4b). Since 3-BP could also act as an alkylating agent towards the –SH groups of NAC, to exclude that the restored levels of GSH after NAC treatment are not due to GSH synthesis from cysteine, but to the lack of 3-BP, GAPDH activity was assayed as main 3-BP target enzyme. As shown by the typical experimental traces reported in Fig. 4c, we found that after 24 h of incubation with 3-BP, GAPDH activity was still significantly inhibited in NAC-pre-treated PC-3 cells (70 ± 5 % of inhibition as compared to control cells, $P < 0.05$), this showing that NAC does not sequester 3-BP inside the cell.

The observed 3-BP-dependent impairment of GAPDH activity might favour the formation of the highly reactive aldehyde MG (Kalapos 1999; Rabbani and Thornalley 2015) mainly formed from the glycolytic triose phosphate intermediates and detoxified by the MG pathway (Kalapos 1999) (see Scheme 1). Thus, we checked whether 3-BP could also affect the activity of the MG pathway enzymes. At this aim, GLOI and GLOII activities were assayed in CSFs of PC-3 cells incubated with 3-BP for 24 h and found to be 411 ± 49 and 20.0 ± 2.6 nmol/min x mg protein, respectively, significantly inhibited as compared to control activities (1027 ± 34 and 42.5 ± 2.3 nmol/min x mg protein, respectively) ($P < 0.01$) (Fig. 4d). Time-dependent measurements of GLOI and GLOII activities showed that the inhibition of both the enzyme activities occurred already after 3 h of PC-3 cell incubation with the drug (47 ± 3.1 and 67 ± 3.3 % of the control, respectively, $P < 0.01$) and maintained for all the incubation times (Fig. 4e).

To evaluate the impact of 3-BP-dependent GSH depletion and impairment of MG pathway enzymes on PC-3 cell survival, cells were pre-treated with either NAC, which we show to contribute to cell redox balance (Fig. 4a, b), or AG, a carbonyl scavenger that rapidly reacts with MG (de Arriba et al. 2007), and then incubated for 24 h in the absence or presence of 3-BP (Fig. 4f). 3-BP-induced PC-3 cell death was almost completely prevented by AG (82 ± 3.5 % of control, $P < 0.05$) and fully counteracted by NAC (Fig. 4f).

3-BP induces necrosis in PC-3 cells

The rapid and remarkable decrease of cellular ATP levels, as well as the rapid depletion of GSH pool and increase in cell oxidative stress, would suggest that PC-3 cell death induced by 3-BP might occur via necrosis rather than apoptosis (Eguchi et al. 1997). This was checked directly by photometric enzyme-immunoassay allowing for the detection of both cell necrosis and apoptosis, measured as increase of sample absorbance at the measurement-reference wavelengths of 405–655 nm (see Materials and methods section). Indeed we found that PC-3 cells incubated for 24 h either in the absence or presence of 3-BP at increasing concentrations, mainly underwent necrosis rather than apoptosis (Fig. 5a), starting from 40 μM 3-BP.

Since cells undergoing necrosis typically exhibit rapid swelling and loss of membrane integrity causing L-LDH release (Porcelli et al. 2015), L-LDH activity was assayed in the culture medium of PC-3 cells incubated with 3-BP (50 μM) for increasing incubation times (Fig. 5b). A significant increase in released L-LDH activity was found starting from 3 h of incubation ($P < 0.01$), this further showing the occurrence of cell necrosis, whereas no significant increase in L-LDH activity was detected at 1 h of incubation, when no effect on cell viability occurred (Fig. 1c, d).

Discussion

The peculiar energy metabolism of prostate cancer cells, in which both glycolysis and functional mitochondria concur to an efficient ATP production and, ultimately, to cell growth and proliferation (Liu 2006; Franklin and Costello 2007; Matheson et al. 2007; de Bari et al. 2010; de Bari et al. 2013; Panov and
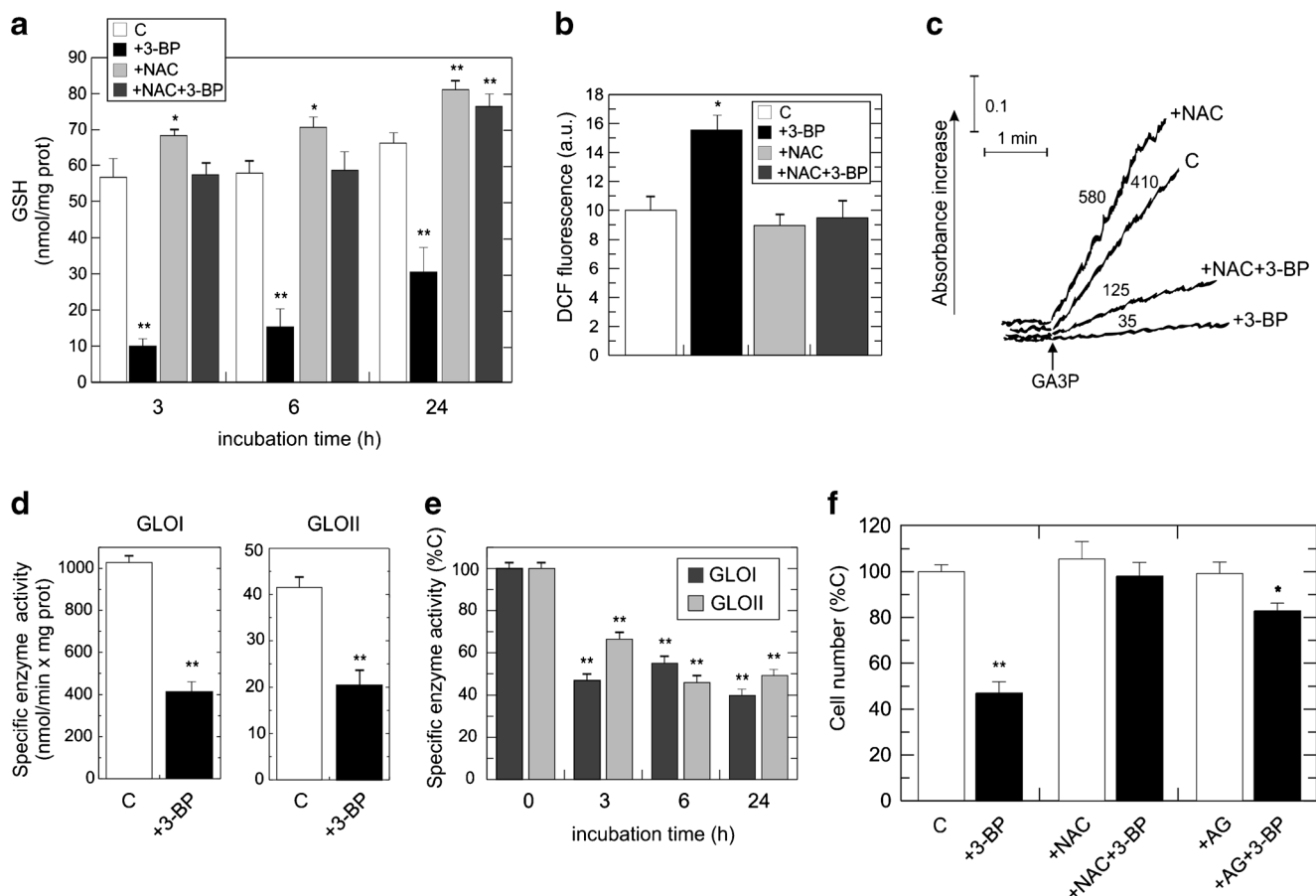
Fig. 4 3-BP treatment causes the depletion of GSH level, the increase in intracellular ROS level and impairment of GLOI and GLOII activity of PC-3 cells. (**a,b**) PC-3 cells (about 2.5–3.0 × 10^6 cells) were pre-incubated in the absence (C) or presence of 1 mM NAC and then the medium (10 ml) was replaced with the same volume of either 3-BP (50 μM)-containing medium (+3-BP, +NAC + 3-BP,) or 3-BP-free medium (C, +NAC), for the reported incubation times (**a**) or for 3 h (**b**), as described in the Material and methods section. (**a**) GSH level, expressed as nmol/mg of CSF protein, was measured photometrically in CSFs isolated from PC-3 cells. Values represent means ± SD (*n* = 4). (**b**) The quantification of intracellular ROS in PC-3 cells was carried out fluorimetrically by staining cells with 5 μM DCF-DA, as described in the Materials and methods section. Values are the means ± SD (*n* = 3) of DCF fluorescence arbitrary units (a.u.). (**c**) The activity of GAPDH was assayed as described in Fig. 2c and in the Materials and methods section, in CSF (0.06 mg protein) of PC-3 cells pre-treated (+NAC) or not (C) with NAC (1 mM) and then incubated either in the absence (C, +NAC) or

presence of 50 μM 3-BP (+3-BP, +NAC + BP) for 24 h. Glyceraldehyde 3-phosphate (GA3P, 3 mM) was added to start the reaction. Numbers along the traces are specific enzyme activities measured as tangent to the initial part of the progress curve and expressed as nmol/min x mg of CSF protein. (**d,e**) The activity of GLOI and GLOII was assayed photometrically in CSFs of PC-3 cells incubated either in the absence (C) or presence of 50 μM 3-BP (+3-BP) for 24 h (**d**) or for the reported incubation times (**e**) and expressed as nmol/min x mg protein (**d**), or % of time-matched controls (**e**). Values represent means ± SD (*n* = 5). (**f**) Cell number was analysed by Trypan Blue exclusion assay. PC-3 cells were pre-incubated in the absence (C) or presence of either 1 mM NAC (+NAC) or 0.5 mM AG (+AG) and then the medium was replaced with either 3-BP (50 μM)-containing medium (+3-BP, +NAC + 3-BP, +AG + 3-BP) or fresh medium (C, +NAC, +AG), for 24 h. Values are means ± SD (*n* = 3) of cell numbers expressed as % of the untreated control (C). ***P* < 0.01 and **P* < 0.05, significantly different from untreated cells

Orynbayeva 2013), prompted us to test in cultured human prostate cancer cells, the effect of 3-BP, known to deplete cell energy reserves by acting on both glycolytic and mitochondrial targets (Shoshan 2012; Galina 2014). It should be noted that recently 3-BP, properly formulated for the delivery in humans, has been successfully administrated to a patient affected by advanced fibrolamellar hepatocellular carcinoma, with low side effects on normal tissues (Ko et al. 2012).

We show that 3-BP rapidly kills both androgen-insensitive and androgen-responsive prostate cancer cells at micromolar concentrations, with the more aggressive, metastatic tumor-

derived PC-3 cells being more sensitive to 3-BP than LNCaP cells. This apparent 3-BP selectivity in prostate cancer cells, could be attributed to the already reported overexpression of monocarboxylate translocators (MCTs) in PC-3 as compared to LNCaP cells (Pértega-Gomes et al. 2011; Vaz et al. 2012; Pértega-Gomes et al. 2013; Pértega-Gomes and Baltazar 2014), which could account to a more efficient uptake of 3-BP (Amoêdo et al. 2013; Ganapathy-Kanniappan et al. 2013) by PC-3 cells (see Scheme 1). Of course further studies are required to verify this; however if so, 3-BP might give good outcomes in the treatment of aggressive, drug-
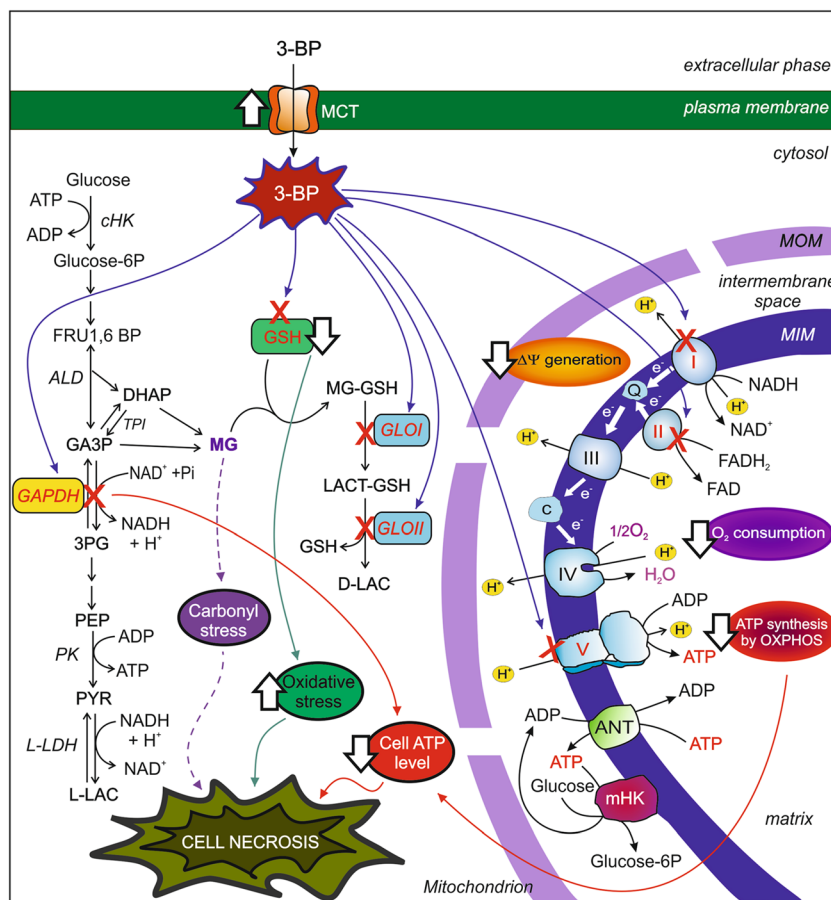
Scheme 1 The multi-target 3-BP cytotoxic action in prostate cancer cells. The multi-target cytotoxic action of 3-BP in PC-3 cells is shown. 3-BP can enter prostate cancer cells likely by the monocarboxylate translocators (MCT), shown to be highly expressed (⬆) in PC-3 cells. Once in the cytosol, 3-BP can directly react with GAPDH and GSH, causing the inhibition (✖) of GAPDH activity and the depletion of GSH pool (⬇). This, in turn, can contribute (*grey solid lines*) to the observed decrease in cell ATP level (⬇) and increase in oxidative stress (⬆), respectively. On the other hand, 3-BP-dependent inhibition of both GLOI and GLOII activity occurs; the glyoxalase system inhibition, together with GAPDH inhibition and GSH depletion, probably contributes to a condition of MG-dependent carbonyl stress, which might contribute to prostate cancer cell death (see text for details).

Dotted grey lines indicate processes that require further investigations. 3-BP also targets mitochondrial functions: 3-BP-dependent inhibition (✖) of MRC complexes I, II and V activity and impairment (⬇) of mitochondrial $\Delta\psi$ generation, oxygen consumption and ATP synthesis by OXPHOS occur, contributing to the decrease of cell ATP level. **Other abbreviations not reported in the text**: ALD, aldolase; ANT, adenine nucleotide translocator; FRU1,6 BP, fructose 1,6 bisphosphate; PEP, phosphoenolpyruvate; 3PG, 1,3-bisphosphoglycerate; L-, D-LAC, L-, D-lactate; LACT-GSH, lactoylglutathione; MG-GSH, glutathione-MG hemithioacetal; MIM, mitochondrial inner membrane; MOM, mitochondrial outer membrane; PYR, pyruvate; TPI, triose phosphate isomerase. **Respiratory chain complexes:** I, NADH:ubiquinone oxidoreductase; II, succinate dehydrogenase; Q, coenzyme Q; III, cytochrome c oxidoreductase; c, cytochrome c; IV, cytochrome oxidase; V, ATP synthase; e⁻, electrons

resistant human prostate cancer in which MCTs overexpression has been proposed as a biomarker and associated with poor prognosis (Pértega-Gomes et al. 2011; Pértega-Gomes et al. 2013; Pértega-Gomes and Baltazar 2014).

The present functional study sheds light on the killing mechanisms and cell metabolic alterations following the treatment of human prostate cancer cells with 3-BP, to our knowledge never examined before. We found that early 3-BP targets in PC-3 cells are: i) the glycolytic enzyme GAPDH, resulting in a strong reduction of its activity, ii) mitochondria, with the impairment of MRC complexes and OXPHOS, iii) GSH, resulting in a

remarkable reduction of GSH cell pool; iv) glyoxalase system (see Scheme 1). This 3-BP multimodal action, leading to an early marked reduction of cellular ATP levels and a significant increase in oxidative stress, rapidly induces PC-3 cell death by necrosis (see Scheme 1). The 3-BP-dependent cytotoxic events occurring in PC-3 cells are discussed separately below.

GAPDH inhibition by 3-BP has been already reported in different cancer cell types (Ganapathy-Kanniappan et al. 2013). Here we further show that a direct interaction between 3-BP and GAPDH occurs causing its inhibition, in agreement with Ganapathy-Kanniappan et al. (2009) who reported 3-BP-
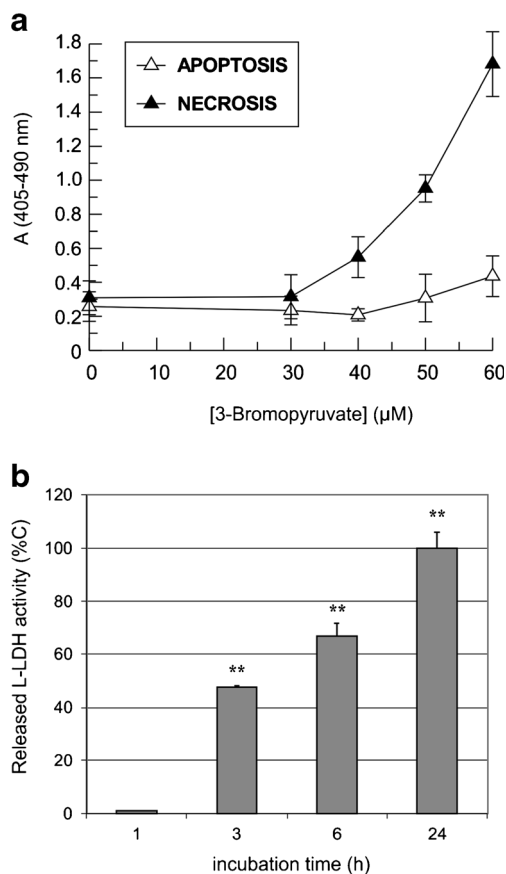
a

b

Fig. 5 3-BP treatment induces PC-3 cell necrosis. (**a**) PC-3 cells were seeded into 96-well plate and treated for 24 h with 3-BP at the indicated concentrations. Apoptosis and necrosis were detected photometrically by the Cell Death Detection ELISA assay at the measurement-reference wavelength of 405–490 nm, respectively, as described in the Materials and methods section. (**b**) L-LDH activity was assayed in the culture medium of PC-3 cells incubated with 3-BP (50 μM) for the reported incubation times, as described in the Materials and methods section. Results represent means ± SD ($n = 3$) and are expressed as percent of maximum L-LDH activity released by 3-BP-treated cells at 24 h (100 %). *$P < 0.01$, significantly different from the activity found in the culture medium of untreated cells

mediated pyruvylation of GAPDH in human hepatocellular carcinoma cells. On the contrary, no 3-BP-dependent inhibitory effect was found in PC-3 cells on the activities of other glycolytic enzymes such as cHK, mHK, PK and L-LDH. Interestingly, mitochondrial membrane-associated mHK activity, assayed here for the first time in mitochondrial membrane enriched fractions isolated from cultured cells, was found increased rather than impaired, this indicating that 3-BP treatment did not cause neither the inhibition nor the detachment of the enzyme from the membrane. Thus, we can hypothesize that 3-BP could impair the entry of triose phosphate intermediates in the ATP-producing phase of glycolysis, without affecting glucose phosphorylation (see Scheme 1). Furthermore, we found that 3-BP can be reduced by L-LDH, very active in PC-3 cells (de Bari et al. 2010; Vaz et al. 2012), as photometrically detected in CSF of untreated PC-3 cells

added with NADH and 3-BP, used as L-LDH substrate (not shown). Further investigations are required to check whether the product of 3-BP reduction by L-LDH, namely 3-bromolactate, can also exert cytotoxic effects.

Besides the strong impairment of GAPDH activity, 3-BP also impairs mitochondrial bioenergetics in PC-3 cells, here investigated in detail. NADH:ubiquinone oxidoreductase (complex I), succinate dehydrogenase (complex II) and ATP synthase (complex V) activities were significantly inhibited, as compared to untreated cells, already after 3 h of cell incubation (Table 1). Consistently, a remarkable decrease occurred in both GLU/MAL- and SUCC-dependent oxygen consumption rate, mitochondrial Δψ extent and mitochondrial ATP synthesis, in 3-BP-treated cells.

As a result of the impairment of prostate cancer cell bioenergetics, a severe cellular ATP deficit rapidly takes place in 3-BP-treated cells. Thus, it is not surprising that 3-BP induces mostly necrosis rather than apoptosis in PC-3 cells, as already found in human fibrolamellar hepatocellular carcinoma (Ko et al. 2012) and melanoma cell lines (Qin et al. 2010).

On the other hand, the rapid cytotoxic effect of 3-BP is strictly linked to its ability to deplete GSH levels (about 80 % of decrease after 3 h of incubation), increasing cell oxidative stress. Since a multitude of cellular processes relies on proper redox integrity, it is not surprising that PC-3 cell pre-treatment with *N*-acetylcysteine, an agent contributing to cell redox balance, completely prevents 3-BP-induced PC-3 cell death, in line with the results obtained in 3-BP-treated melanoma cell lines (Qin et al. 2010).

Importantly, 3-BP also significantly inhibits both GLOI and GLOII activity, thus probably disrupting cell detoxification capacity. Indeed, in preliminary experiments carried out on 3-BP-treated PC-3 cells, we found about 40 % of decrease in the cytosolic level of D-LAC after 24 h of incubation with the drug, indicative of 3-BP-dependent reduction of the flux through the MG pathway (not shown). It is well established that MG-dependent carbonyl stress (Rabbani and Thornalley 2015) occurs under pathological conditions as a result of decreased GSH level (Münch et al. 2003), reduced glyoxalases activity (Kuhla et al. 2007), or elevation of triosephosphate level (Thornalley et al. 2001; Ahmed et al. 2003), conditions also occurring in 3-BP treated cells. It should be noted that MG could itself induce cell energy deficit by both glycolysis inhibition and mitochondrial respiration impairment, as well as depletion of GSH pool and cell oxidative stress (Biswas et al. 1997; de Arriba et al. 2007; Ghosh et al. 2011; Seo et al. 2014). The occurrence of 3-BP-dependent impairment of MG detoxification pathway and its importance in 3-BP-induced cell death are shown by the almost complete prevention of PC-3 cell death by AG, a carbonyl scavenger shown to protect cells from MG cytotoxicity (de Arriba et al. 2007). Further investigations are needed to detect how MG might contribute to 3-BP-induced cell death.

In conclusion, the present report suggests that, on the basis of the combined inhibitory action of 3-BP on cellular ATP-producing pathways, and on antioxidant and detoxifying capacity, rapidly causing prostate cancer cell death, 3-BP might be considered as a valid candidate for the treatment of human prostate cancer.

Compliance with ethical standards

Conflicts of interest The authors declare that they have no financial interests or potential conflict of interests regarding the publication of the present paper.

References

Ahmed N, Battah S, Karachalias N, Babaei-Jadidi R, Horányi M, Baróti K, Hollan S, Thornalley PJ (2003) Increased formation of methylglyoxal and protein glycation, oxidation and nitrosation in triosephosphate isomerase deficiency. Biochim Biophys Acta 1639:121–132. doi:10.1016/j.bbadis.2003.08.002

Amoêdo ND, Valencia JP, Rodrigues MF, Galina A, Rumjanek FD (2013) How does the metabolism of tumour cells differ from that of normal cells. Biosci Rep 33:e00080. doi:10.1042/BSR20130066

Antognelli C, Mezzasoma L, Fettucciari K, Mearini E, Talesa VN (2012) Role of glyoxalase I in the proliferation and apoptosis control of human LNCaP and PC3 prostate cancer cells. Prostate 73:121–132. doi:10.1002/pros.22547

Antognelli C, Mezzasoma L, Fettucciari K, Talesa VN (2013) A novel mechanism of methylglyoxal cytotoxicity in prostate cancer cells. Int J Biochem Cell Biol 45:836–844. doi:10.1016/j.biocel.2013.01.003.

Bénit P, Goncalves S, Philippe Dassa E, Brière JJ, Martin G, Rustin P (2006) Three spectrophotometric assays for the measurement of the five respiratory chain complexes in minuscule biological samples. Clin Chim Acta 374:81–86. doi:10.1016/j.cca.2006.05.034

Bernt E, Bergmeyer HU (1963) Lactate dehydrogenase. In: Bergmeyer HU (ed) Methods of enzymatic analysis. Academic Press, London, pp. 736–741

Biswas S, Ray M, Misra S, Dutta DP, Ray S (1997) Selective inhibition of mitochondrial respiration and glycolysis in human leukaemic leucocytes by methylglyoxal. Biochem J 323:343–348

Bobba A, Amadoro G, Valenti D, Corsetti V, Lassandro R, Atlante A (2013) Mitochondrial respiratory chain complexes I and IV are impaired by β-amyloid via direct interaction and through complex I-dependent ROS production, respectively. Mitochondrion 13:298–311. doi:10.1016/j.mito.2013.03.008

Brand MD, Nicholls DG (2011) Assessing mitochondrial dysfunction in cells. Biochem J 435:297–312. doi:10.1042/BJ20110162

Davidson SD, Milanesa DM, Mallouh C, Choudhury MS, Tazaki H, Konno S (2002) A possible regulatory role of glyoxalase I in cell viability of human prostate cancer. Urol Res 30:116–121

de Arriba SG, Stuchbury G, Yarin J, Burnell J, Loske C, Münch G (2007) Methylglyoxal impairs glucose metabolism and leads to energy depletion in neuronal cells-protection by carbonyl scavengers. Neurobiol Aging 28:1044–1050. doi:10.1016/j.neurobiolaging.2006.05.007

de Bari L, Chieppa G, Marra E, Passarella S (2010) L-lactate metabolism can occur in normal and cancer prostate cells via the novel mitochondrial L-lactate dehydrogenase. Int J Oncol 37:1607–1620. doi:10.3892/ijo_00000815

de Bari L, Moro L, Passarella S (2013) Prostate cancer cells metabolize d-lactate inside mitochondria via a D-lactate dehydrogenase which is more active and highly expressed than in normal cells. FEBS Lett 587:467–473. doi:10.1016/j.febslet.2013.01.011

Eguchi Y, Shimizu S, Tsujimoto Y (1997) Intracellular ATP levels determine cell death fate by apoptosis or necrosis. Cancer Res 57:1835–1840

Ehrke E, Arend C, Dringen R (2015) 3-bromopyruvate inhibits glycolysis, depletes cellular glutathione, and compromises the viability of cultured primary rat astrocytes. J Neurosci Res 93:1138–1146. doi:10.1002/jnr.23474

Franklin RB, Costello LC (2007) Zinc as an anti-tumor agent in prostate cancer and in other cancers. Arch Biochem Biophys 463:211–217. doi:10.1016/j.abb.2007.02.033

Galina A (2014) Mitochondria: 3-bromopyruvate vs. mitochondria? A small molecule that attacks tumors by targeting their bioenergetic diversity. Int J Biochem Cell Biol 54:266–271. doi:10.1016/j.biocel.2014.05.013

Ganapathy-Kanniappan S, Geschwind JF, Kunjithapatham R, Buijs M, Vossen JA, Tchernyshyov I, Cole RN, Syed LH, Rao PP, Ota S, Vali M (2009) Glyceraldehyde-3-phosphate dehydrogenase (GAPDH) is pyruvylated during 3-bromopyruvate mediated cancer cell death. Anticancer Res 29:4909–4918

Ganapathy-Kanniappan S, Kunjithapatham R, Geschwind JF (2013) Anticancer efficacy of the metabolic blocker 3-bromopyruvate: specific molecular targeting. Anticancer Res 33:13–20

Geschwind JF, Ko YH, Torbenson MS, Magee C, Pedersen PL (2002) Novel therapy for liver cancer: direct intraarterial injection of a potent inhibitor of ATP production. Cancer Res 62:3909–3913

Ghosh A, Bera S, Ghosal S, Ray S, Basu A, Ray M (2011) Differential inhibition/inactivation of mitochondrial complex I implicates its alteration in malignant cells. Biochemistry (Mosc) 76:1051–1060. doi:10.1134/S0006297911090100

Higgins LH, Withers HG, Garbens A, Love HD, Magnoni L, Hayward SW, Moyes CD (2009) Hypoxia and the metabolic phenotype of prostate cancer cells. Biochim Biophys Acta 1787:1433–1443. doi:10.1016/j.bbabio.2009.06.003

Kalapos MP (1999) Methylglyoxal in living organisms: chemistry, biochemistry, toxicology and biological implications. Toxicol Lett 110:145–175

Kawatani M, Okumura H, Honda K, Kanoh N, Muroi M, Dohmae N, Takami M, Kitagawa M, Futamura Y, Imoto M, Osada H (2008) The identification of an osteoclastogenesis inhibitor through the inhibition of glyoxalase I. Proc Natl Acad Sci U S A 105:11691–11696. doi:10.1073/pnas.0712239105

Ko YH, Pedersen PL, Geschwind JF (2001) Glucose catabolism in the rabbit VX2 tumor model for liver cancer: characterization and targeting hexokinase. Cancer Lett 173:83–91

Ko YH, Smith BL, Wang Y, Pomper MG, Rini DA, Torbenson MS, Hullihen J, Pedersen PL (2004) Advanced cancers: eradication in all cases using 3-bromopyruvate therapy to deplete ATP. Biochem Biophys Res Commun 324:269–275. doi:10.1016/j.bbrc.2004.09.047

Ko YH, Verhoeven HA, Lee MJ, Corbin DJ, Vogl TJ, Pedersen PL (2012) A translational study "case report" on the small molecule "energy blocker" 3-bromopyruvate (3BP) as a potent anticancer agent: from bench side to bedside. J Bioenerg Biomembr 44:163–170. doi:10.1007/s10863-012-9417-4

Koppenol WH, Bounds PL, Dang CV (2011) Otto Warburg's contributions to current concepts of cancer metabolism. Nat Rev Cancer 11:325–337. doi:10.1038/nrc3038

Kuhla B, Boeck K, Schmidt A, Ogunlade V, Arendt T, Münch G, Lüth HJ (2007) Age- and stage-dependent glyoxalase I expression and its activity in normal and Alzheimer's disease brains. Neurobiol Aging 28:29–41. doi:10.1016/j.neurobiolaging.2005.11.007

LeBel CP, Ischiopoulos H, Bondy SC (1992) Evaluation of the probe 2'7'-dichlorofluoerescin as an indicator of reactive oxygen species formation and oxidative stress. Chem Res Toxicol 5:227–231

Liu Y (2006) Fatty acid oxidation is a dominant bioenergetic pathway in prostate cancer. Prostate Cancer Prostatic Dis 9:230–234

Lohr GW, Waller HD (1963) Glucose-6-phosphate dehydrogenase. In: Bergmeyer HU (ed) Methods of enzymatic analysis. Weinheim, Verlag Chemie GmbH, pp. 744–751

Matheson BK, Adams JL, Zou J, Patel R, Franklin RB (2007) Effect of metabolic inhibitors on ATP and citrate content in PC3 prostate cancer cells. Prostate 67:1211–1218. doi:10.1002/pros.20617

Münch G, Kuhla B, Lüth HJ, Arendt T, Robinson SR (2003) Anti-AGEing defences against Alzheimer's disease. Biochem Soc Trans 31:1397–1399

Panov A, Orynbayeva Z (2013) Bioenergetic and antiapoptotic properties of mitochondria from cultured human prostate cancer cell lines PC-3, DU145 and LNCaP. PLoS One 8:e72078. doi:10.1371/journal.pone.0072078

Pereira da Silva AP, El-Bacha T, Kyaw N, dos Santos RS, da-Silva WS, Almeida FC, Da Poian AT, Galina A (2009) Inhibition of energy-producing pathways of HepG2 cells by 3-bromopyruvate. Biochem J 417:717–726. doi:10.1042/BJ20080805

Pértega-Gomes N, Baltazar F (2014) Lactate transporters in the context of prostate cancer metabolism: what do we Know? Int J Mol Sci 15:18333–18348. doi:10.3390/ijms151018333

Pértega-Gomes N, Vizcaíno JR, Miranda-Gonçalves V, Pinheiro C, Silva J, Pereira H, Monteiro P, Henrique RM, Reis RM, Lopes C, Baltazar F (2011) Monocarboxylate transporter 4 (MCT4) and CD147 over-expression is associated with poor prognosis in prostate cancer. BMC Cancer 11:312. doi:10.1186/1471-2407-11-312

Pértega-Gomes N, Vizcaíno JR, Gouveia C, Jerónimo C, Henrique RM, Lopes C, Baltazar F (2013) Monocarboxylate transporter 2 (MCT2) as putative biomarker in prostate cancer. Prostate 73:763–769. doi:10.1002/pros.22620

Porcelli L, Guida G, Quatrale AE, Cocco T, Sidella L, Maida I, Iacobazzi RM, Ferretta A, Stolfa DA, Strippoli S, Guida S, Tommasi S, Guida M, Azzariti A (2015) Aurora kinase B inhibition reduces the proliferation of metastatic melanoma cells and enhances the response to chemotherapy. J Transl Med 13:26. doi:10.1186/s12967-015-0385-4

Principato GB, Rosi G, Talesa V, Giovannini E, Uotila L (1987) Purification and characterization of two forms of glyoxalase II from the liver and brain of wistar rats. Biochim Biophys Acta 911:349–355

Qin JZ, Xin H, Nickoloff BJ (2010) 3-bromopyruvate induces necrotic cell death in sensitive melanoma cell lines. Biochem Biophys Res Commun 396:495–500. doi:10.1016/j.bbrc.2010.04.126

Rabbani N, Thornalley PJ (2015) Dicarbonyl stress in cell and tissue dysfunction contributing to ageing and disease. Biochem Biophys Res Commun 458:221–226. doi:10.1016/j.bbrc.2015.01.140

Sadowska-Bartosz I, Bartosz G (2013) Effect of 3-bromopyruvic acid on human erythrocyte antioxidant defense system. Cell Biol Int 37:1285–1290. doi:10.1002/cbin.10160

Seo K, Ki SH, Shin SM (2014) Methylglyoxal induces mitochondrial dysfunction and cell death in liver. Toxicol Res 30:193–198. doi:10.5487/TR.2014.30.3.193

Shoshan MC (2012) 3-bromopyruvate: targets and outcomes. J Bioenerg Biomembr 44:7–15. doi:10.1007/s10863-012-9419-2

Thornalley PJ, Jahan I, Ng R (2001) Suppression of the accumulation of triosephosphates and increased formation of methylglyoxal in human red blood cells during hyperglycaemia by thiamine in vitro. J Biochem 129:543–549

Valenti D, Tullo A, Caratozzolo MF, Merafina RS, Scartezzini P, Marra E, Vacca RA (2010) Impairment of F1F0-ATPase, adenine nucleotide translocator and adenylate kinase causes mitochondrial energy deficit in human skin fibroblasts with chromosome 21 trisomy. Biochem J 431:299–310. doi:10.1042/BJ20100581

Valenti D, de Bari L, Manente GA, Rossi L, Mutti L, Moro L, Vacca RA (2013) Negative modulation of mitochondrial oxidative phosphorylation by epigallocatechin-3 gallate leads to growth arrest and apoptosis in human malignant pleural mesothelioma cells. Biochim Biophys Acta 1832:2085–2096. doi:10.1016/j.bbadis.2013.07.014

Vaz CV, Alves MG, Marques R, Moreira PI, Oliveira PF, Maia CJ, Socorro S (2012) Androgen-responsive and nonresponsive prostate cancer cells present a distinct glycolytic metabolism profile. Int J Biochem Cell Biol 44:2077–2084. doi:10.1016/j.biocel.2012.08.013

Weiss M, Gümbel D, Hanschmann E, Mandelkow R, Gelbrich N, Zimmermann U, Walther R, Ekkernkamp A, Sckell A, Kramer A, Burchardt M, Lillig CH, Stope MB (2015) Cold atmospheric plasma treatment induces anti-proliferative effects in prostate cancer cells by redox and apoptotic signaling pathways. PLoS One 10:e0130350. doi:10.1371/journal.pone.0130350

Yang NC, Ho WM, Chen YH, Hu ML (2002) A convenient one-step extraction of cellular ATP using boiling water for the luciferin-luciferase assay of ATP. Anal Biochem 306:323–327. doi:10.1006/abio.2002.5698